Dynamical interaction effects on the Coulomb explosion of H_2^+ at glancing-angle incidence on solid surfaces

You-Nian Wang
Department of Physics, Dalian University of Technology, Dalian 116023, People's Republic of China

Z. L. Mišković* and Wing-Ki Liu
Department of Physics, Guelph-Waterloo Program for Graduate Work in Physics (GWP), University of Waterloo, Waterloo, Ontario, Canada N2L 3G1

(Received 17 December 1997)

The dynamical interaction effects on the Coulomb explosion and the stopping power are studied for MeV H_2^+ ions in grazing collisions with a solid surface. The surface dynamical potential induced by the molecular ions is obtained by using a local frequency-dependent dielectric function for a semi-infinite electron gas with damping. A set of equations describing the motion of the center of mass and the Coulomb explosion is obtained by including the repulsive force of the surface atoms, the bare Coulomb force, and the dynamical forces. The total energy loss for the molecular ion is calculated, taking into account a contribution from both the collective excitations of the conduction electrons and the single-electron excitations of each of the substrate atoms. [S1050-2947(98)03908-0]

PACS number(s): 34.50.Bw, 34.50.Dy, 61.80.−x

I. INTRODUCTION

When a swift molecular ion impinges on a solid, it will dissociate inside the solid and decompose into fragment ions. The resulting ionic fragments then begin to recede from one another under the influence of the bare Coulomb force and separate after a few femtoseconds. This is called ''Coulomb explosion'' of the molecule. The energy loss of the molecular ion in the solid shows important differences—called ''vicinage effects''—when compared with the energy loss of the separated ions. The origin of these effects is due to the interference of the electronic excitations of the solid arising from the correlated motions of the ionic fragments. The existence of the vicinage effects in the energy loss of molecular hydrogen ions in solid carbon was first demonstrated by Brandt *et al.* [1].

What will happen when a fast molecular ion is incident on a solid surface at a small glancing angle? In this case, the molecular ion does not penetrate into the solid but will dissociate into ionic fragments in the region close to the surface before being reflected specularly. The motion of the molecular ion will be influenced not only by the bare Coulomb force, but also by the repulsive force of the surface atoms and the dynamical forces due to the surface electronic excitations. Generally, the course of the Coulomb explosion for the molecular ions moving near the surface is more complex than that inside the solid.

Dissociations of MeV H_2^+ and HeH^+ ions at glancing-angle incidence on solid surfaces were first measured by Susuki *et al.* [2,3]. Similar measurements were also made by Winter *et al.* [4,5]. Subsequently, Susuki *et al.* [6,7] reported on the results of a computer simulation of the dissociation dynamics, in which more than 10^4 particle trajectories were calculated. These experimental measurements and numerical simulations show that almost all molecular ions have dissociated during the scattering, and the internuclear vector of the ionic fragments tends to lie parallel to the surface during dissociation.

Susuki has recently measured energy losses of the H^+ fragments from glancing-angle scattering of 0.15–0.6 MeV/amu H_2^+ ions by SnTe [8] and observed the vicinage effects. He also calculated the energy losses from the collective excitations of the substrate using a local dielectric function with no damping. Although the results agree fairly well with the experimental data, without damping of the plasmon mode the vicinage effects in these calculations do not disappear in the limit of large internuclear distances. For solids such as Si, the damping effect of the high-frequency oscillations of the surface electron-gas should be included [9]. In this case, the vicinage effects will vanish for large internuclear separation, as expected physically.

The main purpose of the present work is to study in detail the dynamical interaction effects on the Coulomb explosion and the stopping power of fast H_2^+ ions during grazing scattering from solid surfaces. We expect that the damping effects in collective excitations will play an important role in the phenomena. The organization of this paper is as follows: In Sec. II, we give the expressions for the surface induced potential of a H_2^+ ion moving near a solid surface using the specular reflection model and a local frequency-dependent dielectric function with damping. In Sec. III, we present the equations of motion describing the scattering of the center of mass and the Coulomb explosion of the molecular ion. The repulsive force of the surface atoms, the bare Coulomb force, and the dynamical forces from surface collective excitations are included. The vicinage effects on the stopping power and

*Also at Department of Applied Mathematics, University of Waterloo, Waterloo, Ontario, Canada N2L 3G1.

 © 1998 The American Physical Society

the total energy loss are discussed in Sec. IV. A summary will be given in Sec. V. Atomic units (a.u.) ($m_e=\hbar=e=1$) will be used throughout this work.

II. SURFACE-INDUCED POTENTIAL

Consider a swift H_2^+ ion incident on a solid surface with a small glancing angle θ_i and reflected specularly. We shall assume that the internuclear vector **R** of the molecular ion is parallel to the surface and aligns with the direction of the projectile's velocity **v**. This assumption is based on the experimental findings [2–5] and numerical simulations [6–8]. Physically, when the molecular ion moves near the solid surface, it will be influenced by both the repulsive force of the surface atoms and the wake force due to the dynamic response of the substrate conduction electrons. The former will orient the internuclear vector parallel to the surface, while the latter will result in the alignment of the internuclear vector along the velocity vector. Even though it is difficult at present to give a quantitative estimate of the time scale for this alignment, one may expect that the extreme grazing conditions will enable the alignment to settle along the incoming trajectory, before the dissociation of H_2^+. We will study the motion of the molecular ion in the x-z plane where the x axis is parallel to the surface and the internuclear vector **R**. The origin of the z coordinate is located on the surface atomic plane, with the solid lying on the $z\leqslant 0$ region.

The angle of incidence for MeV H_2^+ ions on surfaces is about 1–10 mrad in most experiments and the normal component v_z of the velocity **v** is very small. Thus, we can neglect v_z in the calculation of the surface-induced potential and the stopping power, and treat the separation z_c between the ion and the surface adiabatically along the trajectory. The charge density of the molecular ion can be expressed as

$$\rho_{\rm ext}(x,y,z,t)=[\delta(x_1-vt)+\delta(x_2-vt)]\delta(y)\delta(z-z_c), \tag{1}$$

where $x_1=x-R$, $x_2=x$, with the labels 1 and 2 corresponding to the leading ion and the trailing ion in the molecular ion, respectively, and z_c is the instantaneous distance of the ion from the surface atomic plane, considered to be a constant parameter in the calculation of the surface induced potential.

The surface electronic excitations can be described by the well-known specular-reflection model (SRM) introduced by Ritchie and Marusak [10]. The SRM assumes that the solid is a semi-infinite jellium (the electron gas), which is described by a bulk dielectric function $\varepsilon(k,\omega)$. This model has been used by many authors to study the surface-induced potential and the stopping power for atomic ions moving near solid surfaces [11–17]. In the present work, we will use a local frequency-dependent dielectric function

$$\varepsilon(k,\omega)=1-\frac{\omega_p^2}{\omega(\omega+i\gamma)}, \tag{2}$$

where $\omega_p=(4\pi n_0)^{1/2}$ is the plasma frequency of the electron gas with density n_0 and γ is the damping parameter of the electron-gas oscillations. Using the SRM, the surface-induced potential $\Phi(\tilde{x},0,z)$ for a single particle moving parallel to the surface along the x direction with velocity v and distance z_c from the surface can be derived following the procedure of Refs. [11,12]:

$$\Phi(\tilde{x},0,z)=H(\tilde{x},z'_+,\omega_s)+\theta(-z')\theta(-z'_0)[H(\tilde{x},z'_-,\omega_p)-H(\tilde{x},z'_+,\omega_p)], \tag{3}$$

$$H(\tilde{x},z'_\pm,\omega_{s,p})=-\frac{\omega_{s,p}}{v}\int_0^\infty dqJ_0\left(\frac{\omega_{s,p}z'_\pm}{v}q\right)\frac{q^2+1}{(q^2+1)^2-(\gamma q/\omega_{s,p})^2}e^{-q\omega_{s,p}|\tilde{x}|/v}+\theta(-\tilde{x})\frac{2\omega_{s,p}^2}{\Omega_{s,p}v}$$
$$\times\int_0^\infty dqqJ_0\left(\frac{\omega_{s,p}z'_\pm}{v}q\right)\frac{a_{s,p}\sin(\Omega_{s,p}\tilde{x}/v)+b_{s,p}\cos(\Omega_{s,p}\tilde{x}/v)}{(q^2+1)^2-(\gamma q/\omega_{s,p})^2}e^{-\gamma|\tilde{x}|/2v}, \tag{4}$$

$$a_{s,p}=q^2+1-\gamma^2/(2\omega_{s,p}^2), \tag{5}$$

$$b_{s,p}=\gamma\Omega_{s,p}/\omega_{s,p}^2, \tag{6}$$

where $\tilde{x}=x-vt$, $\omega_s=\omega_p/\sqrt{2}$ is the surface plasma frequency, $\Omega_{s,p}=\sqrt{\omega_{s,p}^2-\gamma^2/4}$, $z'_+=|z'|+|z'_c|$, $z'_-=|z'-z'_c|$, and J_0 is the Bessel function. Here, the distances $z'=z-d/2$ and $z'_c=z_c-d/2$ are measured from the jellium edge, and d is the lattice spacing between atomic planes parallel to the surface. In our calculation, we choose d to be the average atomic diameter of the substrate. Since the molecular ion, for some large incident angles, can enter the jellium when it approaches the surface, z' or z'_0 may be negative.

One can see from Eq. (4) that the potential for a single particle can be divided into two parts. The first part is a symmetric function of $\tilde{x}$ and decreases exponentially with increasing $|\tilde{x}|$, while the second part is an oscillatory contribution and appears only in the potential behind the particle. For a finite value of damping factor γ, the oscillatory part will decrease rapidly with increasing $|\tilde{x}|$. In the limit $\gamma\rightarrow 0^+$, Eqs. (3)–(6) reduce to the results of Ref. [11] for undamped electron gas oscillations.

Dynamics of Coulomb explosion of the dissociated molecular ion H_2^+ will be described in the subsequent sections by means of the total induced potential $\Phi_{\rm ind}$, expressed as the sum of the potentials induced by two bare protons, viz.,

$$\Phi_{\rm ind}(x,0,z,t)=\Phi(x_1-vt,0,z)+\Phi(x_2-vt,0,z). \quad (7)$$

Strictly speaking, in the stages before dissociative ionization of H_2^+, the total induced potential should take into account the screening by the electron bound in H_2^+. However, it will be shown that the dissociation occurs at relatively large distances from the surface, so that one may expect that the bound electron will have quantitatively little influence on dynamical interactions prior to dissociation, as well as on the total energy losses. Therefore, we consider, in most of our calculations, the molecular ion before dissociation as two bare protons at a fixed distance R_0. However, the effect of the bound electron on the stopping power in the incoming trajectory will be discussed briefly in Sec. IV A, using a simple model.

III. DYNAMICS OF COULOMB EXPLOSION

A. Equation of motion for individual particle

The equation of motion in the laboratory system for the ith particle at $\mathbf{r}_i$ of the molecular ion is

$$m_i\frac{d\mathbf{v}_i}{dt}=\mathbf{F}_{ij}^{(c)}+\mathbf{F}_i^{(p)}+\mathbf{F}_i^{(s)}+\mathbf{F}_{ij}^{(w)} \quad (i=1,2). \quad (8)$$

The forces appearing on the right-hand side (RHS) of this equation are as follows:

(a) $\mathbf{F}_{ij}^{(c)}$ is the bare Coulomb force

$$\mathbf{F}_{ij}^{(c)}=\frac{\mathbf{r}_i-\mathbf{r}_j}{|\mathbf{r}_i-\mathbf{r}_j|^3}. \quad (9)$$

(b) $\mathbf{F}_i^{(p)}$ is a repulsive force produced by surface atoms, which is given by the planar continuum potential $U_p(z)$:

$$\mathbf{F}_i^{(p)}=-\frac{\partial U_p(z_i)}{\partial z_i}\mathbf{e}_z, \quad (10)$$

with $\mathbf{e}_z$ being the unit vector along the positive direction of the z axis. In the present work, we use the Molière's approximation for the Thomas-Fermi screening function, which gives for $U_p(z)$ [18]

$$U_p(z)=2\pi Z_2 N_p a_{\rm TF}\sum_{i=1}^{3}(\alpha_i/\beta_i)e^{-\beta_i z/a_{\rm TF}}, \quad (11)$$

where Z_2 is the atomic number of the substrate atoms, $a_{\rm TF}$ is the Thomas-Fermi screening length, N_p is the atomic density on the atomic plane, $\{\alpha_i\}=\{0.1,0.55,0.35\}$, and $\{\beta_i\}=\{6,1.2,0.3\}$.

(c) $\mathbf{F}_i^{(s)}$ is the stopping force produced by the induced potential of ith particle on itself

$$\mathbf{F}_i^{(s)}=-\left[\frac{\partial\Phi(\tilde{x},0,z)}{\partial x}\mathbf{e}_x+\frac{\partial\Phi(\tilde{x},0,z)}{\partial z}\mathbf{e}_z\right]_{(\tilde{x}=0,\ z=z_i)}, \quad (12)$$

with $\mathbf{e}_x$ being the unit vector along the positive direction of the x axis.

(d) $\mathbf{F}_{ij}^{(w)}$ is the wake force produced by the jth particle and acting on the ith particle

$$\mathbf{F}_{ij}^{(w)}=-\left[\frac{\partial\Phi(\tilde{x},0,z)}{\partial x}\mathbf{e}_x+\frac{\partial\Phi(\tilde{x},0,z)}{\partial z}\mathbf{e}_z\right]_{(\tilde{x}=x_i-x_j,\ z=z_i)}. \quad (13)$$

One can see from Eqs. (4) and (13) that the wake force is not antisymmetric with respect to interchanging the indices of the two particles, i.e., $\mathbf{F}_{12}^{(w)}\neq-\mathbf{F}_{21}^{(w)}$, and hence will not obey Newton's third law.

Kagan *et al.* [19] and Jakas and Capuj [20] presented similar equations in their studies of fast molecular ions moving in solids. They used simple models for the dynamical potentials and the planar continuum potential is absent in the bulk case.

B. Motion of the center of mass

The center-of-mass coordinate and velocity for the molecular ion are given by $\mathbf{r}_c=(m_1\mathbf{r}_1+m_2\mathbf{r}_2)/M_c$ and $\mathbf{v}=(m_1\mathbf{v}_1+m_2\mathbf{v}_2)/M_c$, respectively, where $M_c=m_1+m_2$. For the H_2^+ ion, $m_1=m_2=m_p$ and $M_c=2m_p$ where m_p is the proton mass. As mentioned in the previous section, we assume that the molecular ion is aligned parallel to the x axis so that $z_1=z_2=z_c$. Furthermore, for swift ions at grazing incidence, the x component of the center-of-mass velocity is approximately constant $v_x=v$, $v_x\gg v_z$, and $x_c=vt$. From Eqs. (8)–(13), we obtain

$$M_c\frac{dv_z}{dt}=-2\frac{\partial U_p(z_c)}{\partial z_c}-2\frac{\partial U_s(z_c)}{\partial z_c}-2\frac{\partial U_w(z_c,R)}{\partial z_c}, \quad (14)$$

where

$$U_s(z)=-\frac{\omega_s}{2v}\int_0^{q_c}dq\frac{(q^2+1)J_0(2\omega_s|z'|q/v)}{(q^2+1)^2-(\gamma q/\omega_s)^2}-\theta(-z')\frac{\omega_p}{2v}\times\int_0^{q_c}dq\frac{(q^2+1)[1-J_0(2\omega_p|z'|q/v)]}{(q^2+1)^2-(\gamma q/\omega_p)^2} \quad (15)$$

is the surface image potential for a single particle, and

$$U_w(z,R)=-\frac{\omega_s}{2v}\int_0^{q_c}dq\frac{(q^2+1)J_0(2\omega_s|z'|q/v)}{(q^2+1)^2-(\gamma q/\omega_s)^2}e^{-q(\omega_s R/v)}-\frac{\omega_s^2}{2v\Omega_s}\int_0^{q_c}dqqJ_0\left(\frac{2\omega_s|z'|q}{v}\right)\frac{a_s\sin(\Omega_s R/v)-b_s\cos(\Omega_s R/v)}{(q^2+1)^2-(\gamma q/\omega_s)^2}$$
$$\times e^{-(\gamma R/2v)}-\theta(-z')\frac{\omega_p}{2v}\int_0^{q_c}dq\frac{(q^2+1)[1-J_0(2\omega_p|z'|q/v)]}{(q^2+1)^2-(\gamma q/\omega_p)^2}e^{-q(\omega_p R/v)}-\theta(-z')\frac{\omega_p^2}{2v\Omega_p}\int_0^{q_c}dq$$
$$\times q\left[1-J_0\left(\frac{2\omega_p|z'|q}{v}\right)\right]\frac{a_p\sin(\Omega_p R/v)-b_p\cos(\Omega_p R/v)}{(q^2+1)^2-(\gamma q/\omega_p)^2}e^{-(\gamma R/2v)} \quad (16)$$

is the dynamical image interaction between the two particles [21] with $a_{s,p}$ and $b_{s,p}$ given in Eqs. (5) and (6). We have introduced a cutoff $q_c=v/v_F$ in the upper limits of integrals in Eqs. (15) and (16), where v_F is the Fermi velocity of the electron gas [16,21].

Using $M_c dv_z/dt=d(M_c v_z^2/2)/dz_c$ and completing the z_c integration in Eq. (14), the trajectory of the center of mass can be obtained from

$$\frac{dz_c}{dx_c}=\mp\theta_i\sqrt{1-\frac{2U_p(z_c)+2U_s(z_c)+2U_w(z_c,R)}{E_c\theta_i^2}}, \quad (17)$$

where $E_c=M_c v^2/2$ is the initial kinetic energy of the center of mass, θ_i is the angle of incidence, and $\mp$ correspond to the incoming (IN) and the outgoing (OUT) trajectories, respectively. The distance of closest approach z_m of the center of mass to the surface atomic layer is given by

$$2U_p(z_m)+2U_s(z_m)+2U_w(z_m,R)=E_c\theta_i^2. \quad (18)$$

Before studying in detail the trajectory of the center of mass and the Coulomb explosion, it is necessary to determine the distances z_D from the surface atomic plane where H_2^+ dissociates into H^+ ions. Generally, it is difficult to determine z_D exactly. We shall use qualitative arguments of Susuki [8], based on the probability that H_2^+ survives to the distance z_c from the surface, viz.,

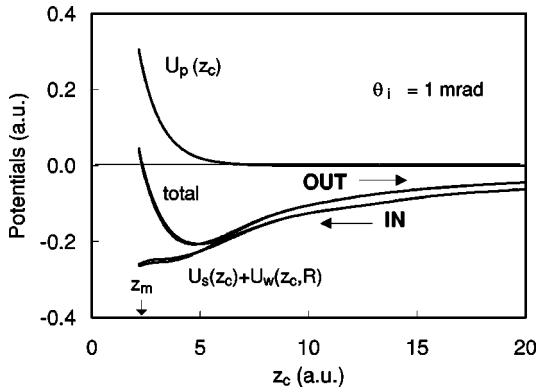

FIG. 1. The potentials governing the center-of-mass motion of a swift H_2^+ ion ($v=5$ a.u. and $\theta_i=1$ mrad) on the Si surface, where $U_p(z_c)$ is planar continuum potential and $U_s(z_c)+U_w(z_c,R)$, are the surface image potentials. The internuclear distance $R(z_c)$ is determined by Eqs. (17), (21), and (22).

$$P_s(z_c)=\exp\left[-\sigma_D(v)\int_\infty^{z_c}dsn(z_c)\right], \quad (19)$$

where s is the path length along the IN trajectory, σ_D is dissociation cross section [22], and $n(z)$ is the electron density outside the surface atomic plane. For glancing incidence, $ds\simeq dx_c=dz_c/(dz_c/dx_c)$ where (dz_c/dx_c) is given by Eq. (17) with the negative sign and R fixed at the initial internuclear distance R_0. Using Eq. (19), z_D is determined from the requirement $P_s(z_c=z_D)=1/e$. The surface electron density $n(z)$ can be derived from the planar continuum potential $U_p(z)$ [see Eq. (11)] using the Poisson equation, yielding

$$n(z)=Z_2N_p/(2a_{\rm TF})\sum_{i=1}^{3}\alpha_i\beta_i e^{-\beta_i z/a_{\rm TF}}. \quad (20)$$

Figure 1 shows the planar-continuum potential $U_p(z_c)$ and the surface image potential $U_s(z_c)+U_w(z_c,R)$ for a swift H_2^+ ion ($v=5$ a.u. and $\theta_i=1$ mrad) on the Si surface ($\omega_s=0.4$ a.u. and $\gamma=0.3$ a.u. [16]). Before the molecular ion dissociates, the internuclear distance R is fixed at the equilibrium bond length R_0, and U_w can be calculated from Eq. (16) with $R=R_0$. When z_c reaches z_D, the molecular ion dissociates, and the internuclear distance R is determined as a function of the distance z_c from the surface (see the following subsection) from the equations describing the Coulomb explosion before substituting into Eq. (16). The planar continuum potential is a short-range repulsive potential and

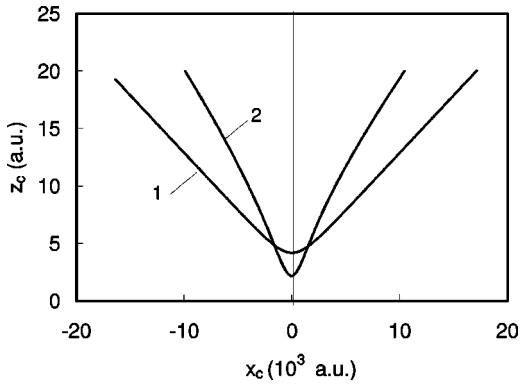

FIG. 2. The trajectories for a swift H_2^+ ion ($v=5$ a.u. and $\theta_i=1$ mrad) on the Si surface, where curve 1 is obtained from the planar continuum potential $U_p(z_c)$ and curve 2 from both the planar continuum potential and the image potentials $U_s(z_c)+U_w(z_c,R)$. The internuclear distance $R(z_c)$ is determined by Eqs. (17), (21), and (22).

the surface image potential is attractive, so that the total potential is negative, except in a region close to the surface.

The center-of-mass trajectory of the molecular ion is shown in Fig. 2. One can see from the figure that the surface image potential makes the ion's flying length shorter than the case when only the planar continuum potential is taken into account. This means that the interaction time of the ion with the solid will be shorter and the Coulomb explosion will be tamed by the surface image potential. In addition, the trajectory is slightly asymmetrical with respect to the z-axis because z_c is a function of the internuclear distance R [see Eq. (17)] and, as shown in the following subsection, the Coulomb explosion is asymmetrical about the z axis.

C. Relative motion

Using Eqs. (8)–(13) again, the equations of motion of the relative coordinate and velocity, $R=x_1-x_2$ and $u=v_1-v_2$, can be put in the following form:

$$\frac{dR}{dx_c}=\frac{u}{v}, \tag{21}$$

$$\frac{du}{dx_c}=\frac{2}{v m_p}[F_c(R)+F_w(z_c,R)], \tag{22}$$

where $F_c(R)=1/R^2$ is the bare Coulomb force and

$$\begin{aligned}F_w(z,R)=&-\frac{\omega_s^2}{v^2}\int_0^{q_c}dqq\frac{(q^2+1)J_0(2\omega_s|z'|q/v)}{(q^2+1)^2-(\gamma q/\omega_s)^2}e^{-q(\omega_s R/v)}+\frac{\omega_s^2}{v^2}\int_0^{q_c}dqqJ_0\left(\frac{2\omega_s|z'|}{v}q\right)\\&\times\frac{(q^2+1)\cos(\Omega_s R/v)-(\gamma/2\Omega_s)(q^2-1)\sin(\Omega_s R/v)}{(q^2+1)^2-(\gamma q/\omega_s)^2}e^{-(\gamma R/2v)}-\theta(-z')\frac{\omega_p^2}{v^2}\int_0^{q_c}dq\\&\times q\frac{(q^2+1)[1-J_0(2\omega_p|z'|q/v)]}{(q^2+1)^2-(\gamma q/\omega_p)^2}e^{-q(\omega_p R/v)}+\theta(-z')\frac{\omega_p^2}{v^2}\int_0^{q_c}dqq\left[1-J_0\left(\frac{2\omega_p|z'|}{v}q\right)\right]\\&\times\frac{(q^2+1)\cos(\Omega_p R/v)-(\gamma/2\Omega_p)(q^2-1)\sin\left(\frac{\Omega_p R}{v}\right)}{(q^2+1)^2-(\gamma q/\omega_p)^2}e^{-(\gamma R/2v)}\end{aligned} \tag{23}$$

is the interacting wake force. After the molecular ion dissociates, Eqs. (17), (21), and (22) must be solved simultaneously to give R, u, and z_c as functions of x_c.

The bare Coulomb force $F_c(R)$ is a strongly repulsive force, while the wake force $F_w(z_c,R)$ is an oscillatory function of R and will be attractive for larger R, especially in the final phase of the Coulomb explosion.

Figure 3 shows the internuclear distance R as a function of the distance z_c from the surface during the Coulomb explosion of a swift H_2^+ ion ($v=5$ a.u. and $\theta_i=1$ mrad) on the Si surface. Comparing the trajectories calculated with and without the wake force, it is obvious that the dynamical effects retard the Coulomb explosion. Hence, in addition to shortening the scattering time of the center of mass as shown in Fig. 2, the dynamical effects also reduce the total force driving the Coulomb explosion. This latter observation can further be seen in Fig. 4, in which the forces driving the relative motion are depicted. In the initial stage of the Coulomb explosion, R is small and the bare Coulomb force $F_c(R)$ is much larger than the wake force $F_w(z_c,R)$. With increasing R in the OUT trajectory, the wake force becomes comparable with the Coulomb force. At about $z_c=6$ the total force is even negative. Thus, the Coulomb explosion will accelerate in the initial stages, but will slow down and even decelerate subsequently with increasing R.

In Fig. 5, we show the influence of the incident angle θ_i on the Coulomb explosion. At the same distance z_c in the OUT trajectories, the Coulomb explosion for the small incident angle is stronger than that for the large incident angle. This is simply due to the longer Coulomb explosion time in the cases of small incidence angles.

IV. VICINAGE EFFECTS

A. Stopping power

We first study the vicinage effects in the stopping power due to collective excitations for swift H_2^+ ions moving near

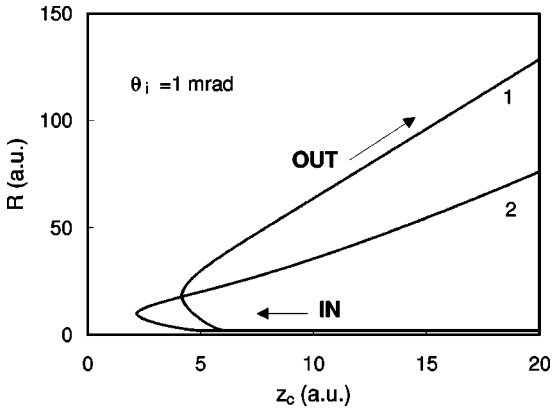

FIG. 3. The Coulomb explosion for a swift H_2^+ ion ($v=5$ a.u. and $\theta_i=1$ mrad) on the Si surface, where curve 1 is obtained from the bare Coulomb force $F_c(R)$, and curve 2 from both the Coulomb force and the wake force $F_w(z_c,R)$. The internuclear distance $R(z_c)$ is determined by Eqs. (17), (21), and (22).

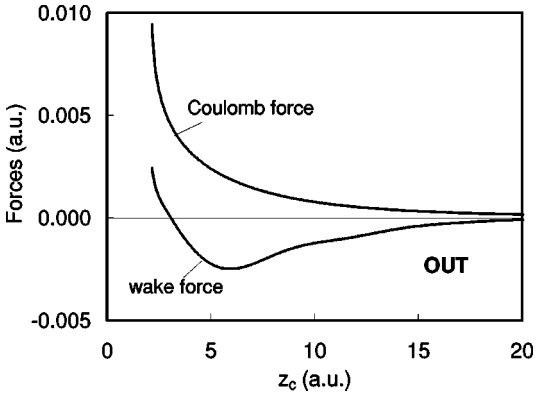

FIG. 4. The forces driving the Coulomb explosion for a swift H_2^+ ion ($v=5$ a.u. and $\theta_i=1$ mrad) on the Si surface, where $F_c(R)$ is the bare Coulomb force and $F_w(z_c,R)$ is the wake force. The internuclear distance $R(z_c)$ is determined by Eqs. (17), (21), and (22).

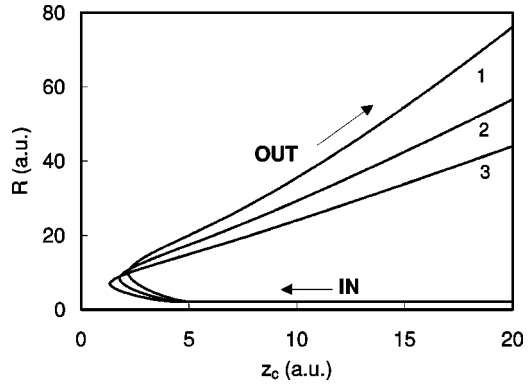

FIG. 5. The dependence on the incident angle of the Coulomb explosion for a swift H_2^+ ion ($v=5$ a.u.) on the Si surface, where curves 1, 2, and 3 correspond to $\theta_i=1$, 2, and 3 mrad, respectively.

solid surface. The vicinage effects were studied by many authors in the bulk case, and we expect this effect will also be important in the surface case. The stopping power for the molecular ion when it is at a distance z_c from the surface layer with internuclear separation R is given by

$$S_{\rm mol}^{(C)}(z_c,R)=-\int d\mathbf{r}\rho_{\rm ext}(x,y,z,t)(-\partial\Phi_{\rm ind}/\partial x). \quad (24)$$

Using Eqs. (1), (3), and (7), we obtain

$$S_{\rm mol}^{(C)}(z_c,R)=2[S_p^{(C)}(z_c)+S_v^{(C)}(z_c,R)], \quad (25)$$

where

$$S_p^{(C)}(z_c)=\frac{\omega_s^2}{v^2}\int_0^{q_c}dqqJ_0(2\omega_s|z_c'|q/v)F(q,0,\omega_s)+\theta(-z_c')\frac{\omega_p^2}{v^2}\int_0^{q_c}dqq[1-J_0(2\omega_p|z_c'|q/v)]F(q,0,\omega_p) \quad (26)$$

is the proton's stopping power due to the collective excitations, and

$$S_v^{(C)}(z_c,R)=\frac{\omega_s^2}{v^2}\int_0^{q_c}dqqJ_0(2\omega_s|z_c'|q/v)F(q,R,\omega_s)+\theta(-z_c')\frac{\omega_p^2}{v^2}\int_0^{q_c}dqq[1-J_0(2\omega_p|z_c'|q/v)]F(q,R,\omega_p) \quad (27)$$

is the vicinage stopping power. The function $F(q,R,\omega_{s,p})$ is given by

$$F(q,R,\omega_{s,p})=-\frac{\gamma q/\omega_{s,p}}{(q^2+1)^2-(\gamma q/\omega_{s,p})^2}e^{-q\omega_{s,p}R/v}+\frac{(q^2+1)\cos(\Omega_{s,p}R/v)-(\gamma/2\Omega_{s,p})(q^2-1)\sin(\Omega_{s,p}R/v)}{(q^2+1)^2-(\gamma q/\omega_{s,p})^2}e^{-\gamma R/2v}. \quad (28)$$

It is easy to see that, when the damping factor $\gamma\to 0$, Eqs. (25)–(28) reduce to Susuki's result [8]

$$S_{\rm mol}^{(C)}(z_c,R)=2\left[1+\cos\left(\frac{\omega_s R}{v}\right)\right]\frac{\omega_s^2}{v^2}\int_0^{q_c}dq\frac{q}{q^2+1}J_0(2\omega_s|z_c'|q/v)+\theta(-z_c')2\left[1+\cos\left(\frac{\omega_p R}{v}\right)\right]\frac{\omega_p^2}{v^2}$$
$$\times\int_0^{q_c}dq\frac{q}{q^2+1}[1-J_0(2\omega_p|z_c'|q/v)]. \quad (29)$$

Note that, in this case, the vicinage effects persist even when $R\to\infty$. On the other hand, for finite $\gamma>0$, Eq. (28) shows that the vicinage effects will disappear as R becomes large.

Only the contributions of the collective excitations to the stopping power are included in the above discussion. When the molecular ion is close to the atomic plane, however, single-electron excitations of the substrate atoms also contribute to the stopping power, especially for large incident angles. The stopping power due to the single-electron excitations can be included by using Bohr's harmonic oscillator model [23]

$$S_{\rm mol}^{(I)}(z_c,R)=2\left[1+\cos\left(\frac{\omega R}{v}\right)\right]S_p^{(I)}, \quad (30)$$

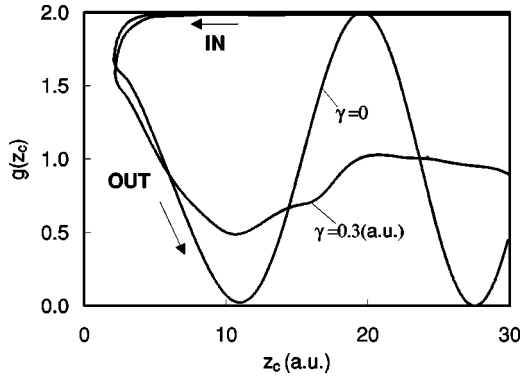

FIG. 6. The effect of damping on the vicinage effects due to the collective excitations for a swift H_2^+ ion ($v=5$ a.u. and $\theta_i=1$ mrad) on the Si surface.

where the harmonic oscillator frequency is given by $\omega(z_c)=[4\pi n(z_c)]^{1/2}$ [24], $n(z)$ is the electronic density from Eq. (20), and

$$S_p^{(I)}(z_c)=\tfrac{1}{2}[\omega(z_c)/v]^2\ln[2v^2/\omega^2(z_c)] \tag{31}$$

is the stopping power of a proton due to the single-electron excitations [24].

The total stopping power for the molecular ion is the sum $S_{\rm mol}=S_{\rm mol}^{(C)}+S_{\rm mol}^{(I)}$, and we define the vicinage function by

$$g(z_c,R)=1+S_{\rm mol}(z_c,R)/[2S_p(z_c)], \tag{32}$$

where $S_p=S_p^{(C)}+S_p^{(I)}$ is the total stopping power of a proton.

In Fig. 6 we plot the vicinage function $g(z_c,R)$ as a function of the distance z_c from the surface for a swift H_2^+ ion ($v=5$ a.u. and $\theta_i=1$ mrad) scattered by a Si surface. Again, the dependence of the internuclear distance R on z_c is obtained by solving Eqs. (17), (21), and (22) simultaneously. We observe that in the OUT trajectory, the vicinage function approaches 1 at the large R limit due to the damping of the collective excitations, while it oscillates rapidly with z_c if we take $\gamma=0$. The influence of the incident angle on the vicinage function is shown in Fig. 7. Consistent with the observation in Fig. 5, for the larger incident angle, Coulomb explosion proceeds more slowly, and the vicinage effect persists for larger value of z_c.

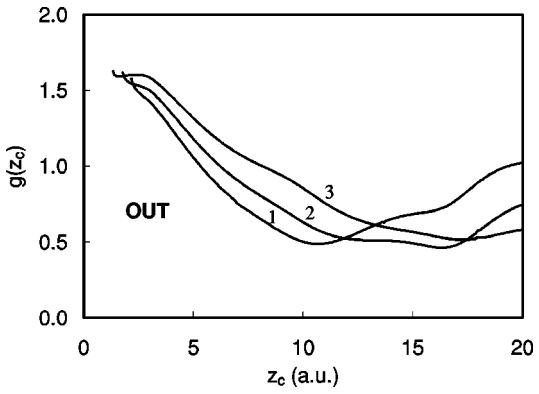

FIG. 7. The dependence on the incident angle of the vicinage effects due to the collective excitations for a swift H_2^+ ion ($v=5$ a.u.) on the Si surface, where curves 1, 2, and 3 correspond to $\theta_i=1,2$, and 3 mrad, respectively.

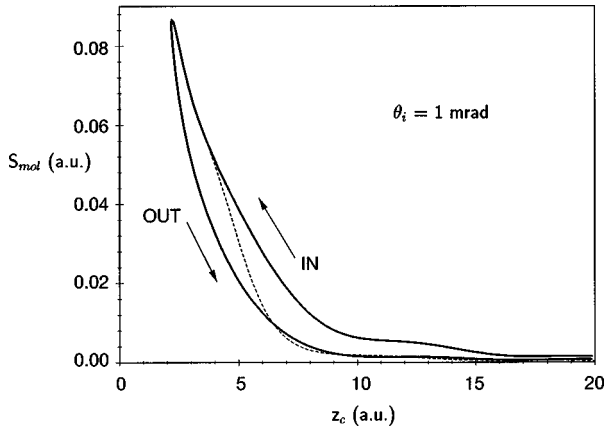

FIG. 8. The total stopping power $S_{\rm mol}$ for a swift H_2^+ ion ($v=5$ a.u. and $\theta_i=1$ mrad) on the Si surface. The dashed line represents the effective stopping power along the IN trajectory, obtained from Eq. (33) (for details see the text).

The total stopping power $S_{\rm mol}=S_{\rm mol}^{(C)}+S_{\rm mol}^{(I)}$ for the molecular ion at $v=5$ a.u. and $\theta_i=1$ mrad is shown in Fig. 8. We find that values of the stopping power in the OUT trajectory are lower than those in the IN trajectory. This is due to the fact that the values of R are generally larger in the latter stages of Coulomb explosion in the OUT trajectory than those in the initial stages in the IN trajectory, and the vicinage function $g(z_c,R)$ decreases in magnitude with R when damping is included.

Let us discuss here the effects of the screening by the bound electron on the stopping power of the molecular ion H_2^+ along the incoming trajectory. To do so, we employ the survival probability $P_s(z_c)$ of H_2^+, Eq. (19), and write for the effective stopping power

$$S_{\rm eff}=P_s(z_c)Z_{\rm eff}^2S_p(z_c)+[1-P_s(z_c)]S_{\rm mol}(z_c), \tag{33}$$

where the stopping power of the molecular ion H_2^+ before dissociation is represented by proton stopping power, weighted by an effective charge $Z_{\rm eff}$. Equation (33) uses the survival probability $P_s(z_c)$ as a switching function between dissociated and undissociated cases of H_2^+. Value of $Z_{\rm eff}$ is largely unknown for surface scattering, and we use Susuki's estimate [8] $Z_{\rm eff}^2=1.4$, based on data on H_2^+ stopping in foils. The effective stopping power $S_{\rm eff}$ along the IN trajectory, Eq. (33), is shown in Fig. 8 by the dashed line. Such a crude model shows that the stopping power of H_2^+ may be affected by the bound electron at large distances where both $S_{\rm mol}$ from our calculations and S_p are small. However, the most prominent contribution to the stopping power comes from shorter distances, after the dissociation, where $S_{\rm mol}$ dominates. Thus, we expect little influence of the bound electron on total energy losses.

B. Energy loss

We study next the vicinage effects in the total energy loss. The total energy loss of the molecular ion H_2^+ can be calculated by integrating the stopping power along the center-of-mass trajectory,

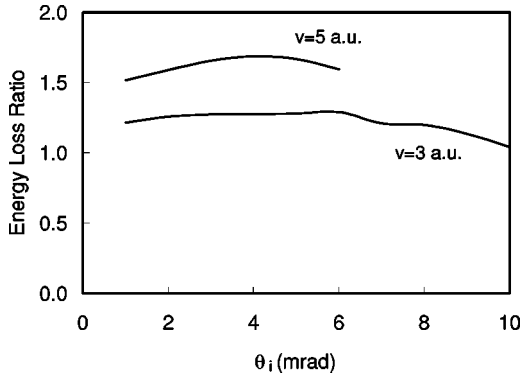

FIG. 9. The ratio of the energy loss $\Delta E_M/(2\Delta E_p)$ for a swift H_2^+ ion ($v=5$ a.u. and $v=3$ a.u.) on the Si surface, where ΔE_p is the energy loss for a proton with the same velocities as the molecular ion.

$$\Delta E_M = \int_0^\infty [S_{\rm mol}^{(\rm IN)}(z_c,R) + S_{\rm mol}^{(\rm OUT)}(z_c,R)]ds, \qquad (34)$$

with $ds=\sqrt{(dx_c)^2+(dz_c)^2}$, where dependences of z_c and R on x_c are determined by the equations of motion (17), (21), and (22).

In Fig. 9 we show the dependence of the energy-loss ratio $\Delta E_M/(2\Delta E_p)$, where ΔE_p is the energy loss of a proton, on the incident angle θ_i for a H_2^+ ion traveling with velocities $v=3$ a.u. and $v=5$ a.u., colliding with the Si surface. Figure 10 shows the dependence of the total energy losses of the molecular ion on the incident angle. These figures reproduce well the magnitude of the experimental data [8] on the energy loss ratio and the total energy loss, respectively. The experiment showed that these quantities are insensitive to the angle of incidence, and our results seem to be in better agreement with this observation than the calculations of Ref. [8]. We believe that this is primarily due to our inclusion of damping in the collective excitations of the electron gas.

V. SUMMARY

We have solved the equations of motion for the Coulomb explosion of a swift H_2^+ ion in grazing scattering from a solid surface, mediated by the dynamic response of the solid electrons. We assume a specific configuration of the H_2^+ ion, where the internuclear vector aligns parallel to the surface in the direction of the center-of-mass motion, which is supported by experimental and computer-simulation findings. Forces governing the center-of-mass motion consist of the repulsive force of the surface atoms, the dynamical self-image forces, as well as the components of the wake forces normal to the surface. The relative motion is driven by the bare Coulomb interaction and the mutual wake interaction.

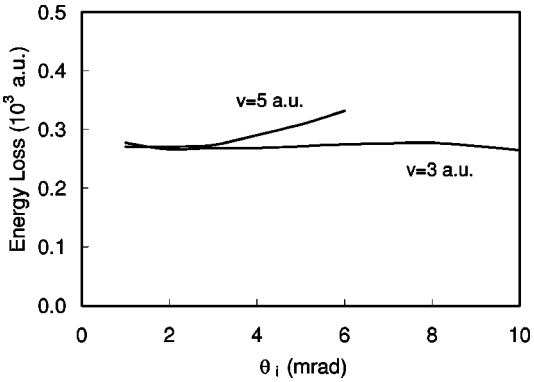

FIG. 10. The energy loss ΔE_M for a swift H_2^+ ion ($v=5$ a.u. and $v=3$ a.u.) on the Si surface.

The energy loss of the H_2^+ ion can be divided into contributions from the independent protons, the vicinage effect, which arises from the interference of the electronic excitations of the substrate by the protons and depends on the internuclear distance, and the single-electron excitations of the substrate atoms.

Collective excitations of the semi-infinite electron gas are described in our calculations by a frequency-dependent dielectric function with damping. Inclusion of damping is important for surfaces such as Si, and produces in the wake forces and the vicinage effects the damped oscillatory behavior as a function of the internuclear separation along the trajectory. As a result, the energy-loss ratio and the total energy loss for Coulomb explosion of a swift H_2^+ ion are almost independent of the angle of incidence in grazing scattering, consistent with experimental observations. Similar effects will be expected when a more complete dielectric function with dispersion is employed.

One of the main uncertainties in our model is the distance z_D from the surface, in the incoming trajectory, at which the Coulomb explosion starts. Using a simple rate-equation approach to the dissociation of H_2^+ on a surface shows that the distances z_D are distributed over a range of order of $a_{\rm TF}$. A complete treatment of this problem is not possible before a detailed scenario of electron transitions, leading to the dissociative ionization of a swift H_2^+ ion, is properly treated.

ACKNOWLEDGMENTS

This work is supported by the National Natural Science Foundation of China (Grant No. 19575008) (Y.N.W.) and by the Natural Sciences and Engineering Research Council (NSERC) of Canada (W.K.L.). Y.N.W. wishes to acknowledge the hospitality of the Department of Physics, University of Waterloo, during his visit, when this research was carried out.

[1] W. Brandt, A. Ratkowski, and R. H. Ritchie, Phys. Lett. **33**, 1325 (1974).

[2] Y. Susuki, H. Mukai, K. Kimura, and M. Mannami, Nucl. Instrum. Methods Phys. Res. B **48**, 347 (1990).

[3] Y. Susuki, H. Mukai, K. Kimura, and M. Mannami, J. Phys. Soc. Jpn. **59**, 1211 (1990).

[4] H. Winter, Radiat. Eff. Defects Solids **117**, 53 (1991).

[5] H. Winter, J. C. Poizat, and J. Remillieux, Nucl. Instrum.

Methods Phys. Res. B **67**, 345 (1992).
[6] Y. Susuki, T. Ito, K. Kimura, and M. Mannami, J. Phys. Soc. Jpn. **61**, 3535 (1992).
[7] Y. Susuki, T. Ito, K. Kimura, and M. Mannami, Phys. Rev. A **51**, 528 (1995).
[8] Y. Susuki, Phys. Rev. A **56**, 2918 (1997).
[9] N. R. Arista, Phys. Rev. A **49**, 1885 (1994).
[10] R. H. Ritchie and A. L. Marusak, Surf. Sci. **4**, 234 (1966).
[11] F. J. García de Abajo and P. M. Echenique, Phys. Rev. B **46**, 2663 (1992).
[12] F. J. García de Abajo and P. M. Echenique, Phys. Rev. B **48**, 13 399 (1993).
[13] G. Gumbs and M. L. Glasser, Phys. Rev. B **37**, 1391 (1988).
[14] P. M. Echenique, F. J. García de Abajo, V. H. Ponce, and M. E. Uranga, Nucl. Instrum. Methods Phys. Res. B **96**, 583 (1995).
[15] Y. N. Wang and W.-K. Liu, Chem. Phys. **254**, 122 (1996).
[16] R. Núñez, P. M. Echenique, and R. H. Ritchie, J. Phys. C **13**, 4229 (1980).
[17] Y. N. Wang and W.-K. Liu, Phys. Rev. A **54**, 636 (1996).
[18] Y. H. Ohtsuki, *Charged Beam Interaction with Solids* (Taylor & Francis, London, 1983).
[19] Y. Kagan, Y. V. Kononets, and N. K. Dzhamankyzoz, Zh. Éksp. Teor. Fiz. **74**, 288 (1978) [Sov. Phys. JETP **47**, 148 (1978)].
[20] M. M. Jakas and N. E. Capuj, Phys. Rev. A **52**, 439 (1995).
[21] T. O'hori and Y. H. Ohtsuki, Phys. Rev. B **27**, 3418 (1983).
[22] D. Mathur, J. B. Hasted, and S. U. Khan, J. Phys. B **12**, 2043 (1979).
[23] J. Basbas and R. H. Ritchie, Phys. Rev. A **25**, 1943 (1982).
[24] Y. Fujii, S. Fujiwara, K. Narumi, K. Kimura, and M. Mannami, Surf. Sci. **227**, 164 (1992).